

**Polydentate N₂S₂O and N₂S₂O₂ Ligands as Alcoholic Derivatives of
(*N,N'*-Bis(2-mercaptoethyl)-1,5-diazacyclooctane)nickel(II) and
(*N,N'*-Bis(2-mercapto-2-methylpropane)-1,5-diazacyclooctane)nickel(II)**

Dawn C. Goodman, Rizalia M. Buonomo, Patrick J. Farmer,[†] Joseph H. Reibenspies, and Marcetta Y. Darensbourg*

Department of Chemistry, Texas A&M University, College Station, Texas 77843-3255

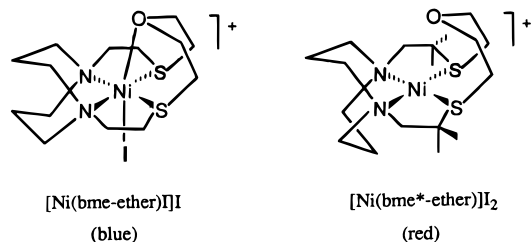
Received November 14, 1995[⊗]

The synthesis, structural characterization, spectroscopic, and electrochemical properties of N₂S₂-ligated Ni^{II} complexes, (*N,N'*-bis(2-mercaptoethyl)-1,5-diazacyclooctane)nickel(II), (bme-daco)Ni^{II}, and (*N,N'*-bis(2-mercapto-2-methylpropane)-1,5-diazacyclooctane)nickel(II), (bme*-daco)Ni^{II}, derivatized at S with alcohol-containing alkyl functionalities, are described. Reaction of (bme-daco)Ni^{II} with 2-iodoethanol afforded isomers, (*N,N'*-bis(5-hydroxy-3-thiapentyl)-1,5-diazacyclooctane-*O,N,N',S,S'*)halonickel(II) iodide (halo = chloro or iodo), **1**, and (*N,N'*-bis(5-hydroxy-3-thiapentyl)-1,5-diazacyclooctane-*N,N',S,S'*)nickel(II) iodide, **2**, which differ in the utilization of binding sites in a potentially hexadentate N₂S₂O₂ ligand. Blue complex **1** contains nickel in an octahedral environment of N₂S₂OX donors; X is best modeled as Cl. It crystallizes in the monoclinic space group *P2₁/n* with *a* = 12.580(6) Å, *b* = 12.291(6) Å, *c* = 13.090(7) Å, β = 97.36(4)°, and *Z* = 4. In contrast, red complex **2** binds only the N₂S₂ donor set forming a square planar nickel complex, leaving both –CH₂CH₂OH arms dangling; the iodide ions serve strictly as counterions. **2** crystallizes in the orthorhombic space group *Pca2₁* with *a* = 15.822(2) Å, *b* = 13.171(2) Å, *c* = 10.0390(10) Å, and *Z* = 4. Reaction of (bme-daco)Ni^{II} with 1,3-dibromo-2-propanol affords another octahedral Ni species with a N₂S₂OBr donor set, ((5-hydroxy-3,7-dithianonadiyl)-1,5-diazacyclooctane-*O,N,N',S,S'*)bromonickel(II) bromide, **3**. Complex **3** crystallizes in the orthorhombic space group *Pca2₁* with *a* = 15.202(5) Å, *b* = 7.735(2) Å, *c* = 15.443(4) Å, and *Z* = 4. Complex **4**·2CH₃CN was synthesized from the reaction of (bme*-daco)Ni^{II} with 1,3-dibromo-2-propanol. It crystallizes in the monoclinic space group *P2₁/c* with *a* = 20.348(5) Å, *b* = 6.5120(1) Å, *c* = 20.548(5) Å, and *Z* = 4.

Introduction

The correlation between a metal's coordination sphere and its redox chemistry has been emphasized in studies aimed at elucidating the catalytic functioning of metalloenzymes. This complexity in properties serves as inspiration for synthetic inorganic chemists to provide small molecule mimics of the structure and function of such enzymes. For the [NiFe] hydrogenases, which contain nickel in a cysteine-sulfur rich environment, either a change in the coordination number of nickel or a charge-neutralization of the thiolate sulfur donor (brought about by protonation or metalation) are possible explanations for the unique redox properties that characterize the enzyme activity.^{1–3} A second example of redox active nickel is in F₄₃₀, which finds nickel in four- or six-coordination, or an equilibrium mixture of both.^{4,5} It is believed that in the six-coordinate species one axial ligand is more tightly bound than the other, thereby being predisposed to a coordination change. Thus, the protein may be able to govern the reactivity of the enzyme by placing the metal in an optimal structural environment for the redox chemistry.^{1,4–6}

The capacity of nickel to bind both hard and soft donor ligands allows its coordination chemistry to encompass a variety of geometries, coordination numbers, and oxidation states with reactivity ranging from that in biological to organometallic chemistry. The (*N,N'*-bis(2-mercaptoethyl)-1,5-diazacyclooctane)nickel(II) complex, (bme-daco)Ni^{II}, has proven to be useful for the synthesis of nickel macrocyclic compounds by taking advantage of the template effect.⁷ The *cis* sulfur sites have led to the preparation of macrocycles with expanded denticity, as in [Ni(bme-ether)I] and [Ni(bme*-ether)]I₂.^{8–11}



In the former complex, the ether oxygen binds to the nickel center forming a six-coordinate product, whereas in the latter, the product is four coordinate. As illustrated, the ether function

[†] Current address: Department of Chemistry, University of California at Irvine, Irvine, CA 92717-2025.

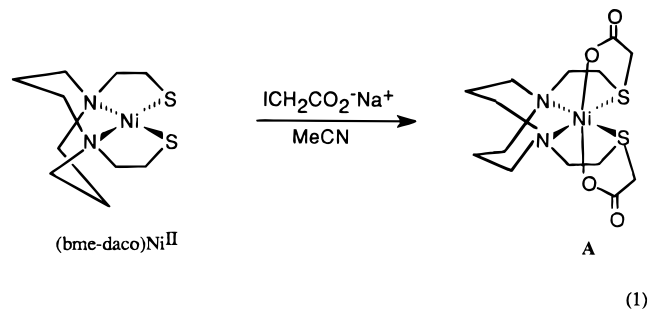
[⊗] Abstract published in *Advance ACS Abstracts*, June 1, 1996.

- (1) Lancaster, J. R., Jr., Ed.; *The Bioinorganic Chemistry of Nickel*; VCH: New York, 1988; Chapters 4 and 12.
- (2) Cammack, R. *Adv. Inorg. Chem.* **1988**, 32, 297.
- (3) Farmer, P. J.; Reibenspies, J. H.; Lindahl, P. A.; Darensbourg, M. Y. *J. Am. Chem. Soc.* **1993**, 115, 4665.
- (4) Eidsness, M. K.; Sullivan, R. J.; Schwartz, J. R.; Hartzell, P. L.; Wolfe, R. D.; Flank, A.-M.; Cramer, S. P.; Scott, R. A. *J. Am. Chem. Soc.* **1986**, 108, 3120.
- (5) Diamun, G. P.; Pigott, B.; Tinton, H. J.; Ankel-Fuchs, D.; Thauer, R. K. *Biochem. J.* **1985**, 232, 281.

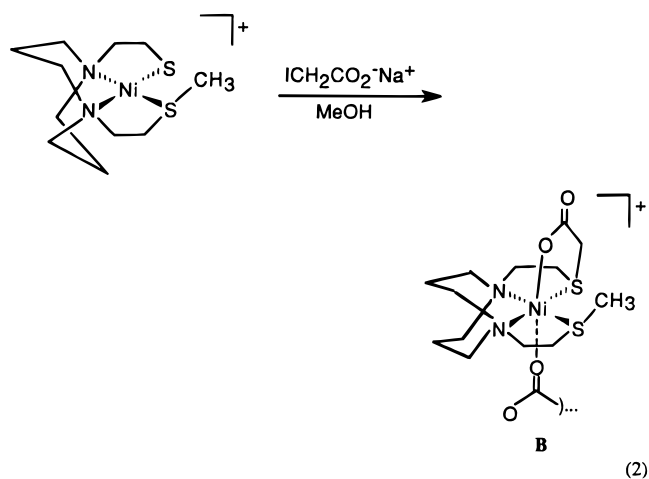
- (6) Kovacs, J. A. *Advances in Inorg. Biochem.* Prentice-Hall: Englewood Cliffs, NJ, 1993; Vol. 9, Chapter 5.
- (7) Thompson, M. C.; Busch, D. H. *J. Am. Chem. Soc.* **1964**, 86, 3651.
- (8) Mills, D. K.; Reibenspies, J. H.; Darensbourg, M. Y. *Inorg. Chem.* **1990**, 29, 4364.
- (9) Goodman, D. C.; Tuntulani, T.; Farmer, P. J.; Darensbourg, M. Y.; Reibenspies, J. H. *Angew. Chem., Int. Ed. Engl.* **1993**, 32, 116.
- (10) Darensbourg, M. Y.; Font, I.; Pala, M.; Reibenspies, J. H. *J. Coord. Chem.* **1994**, 32, 39.
- (11) Darensbourg, M. Y.; Font, I.; Mills, D. K.; Pala, M.; Reibenspies, J. H. *Inorg. Chem.* **1992**, 31, 4965.

on $[\text{Ni}(\text{bme}^*\text{-ether})]_2$ appears situated to readily bind to nickel; however, the axial α -methyl groups provide a steric block toward *trans* iodide binding. Pentacoordination in the $\text{N}_2\text{S}_2\text{O}_{\text{ether}}$ pentadentate ligand has not been observed.

The tendency of nickel to be four- or six-coordinate is further exemplified in the reaction of $(\text{bme-daco})\text{Ni}^{\text{II}}$ with the sodium salt of iodoacetic acid. With stoichiometric or substoichiometric equivalents of $\text{ICH}_2\text{CO}_2\text{Na}$, only the six-coordinate product, **A**, was formed (eq 1).⁹ In an attempt to synthesize the penta-



coordinate $\text{N}_2\text{S}_2\text{O}$ species, one of the sulfurs of $(\text{bme-daco})\text{Ni}^{\text{II}}$ was protected with a methyl group. The subsequent reaction of the monomethyl compound with $\text{ICH}_2\text{CO}_2\text{Na}$ (eq 2) led to



the formation of a blue, coordination polymer, **B**, whose crystal structure shows the nickel interacting strongly with a distal O from an adjacent molecule to complete its octahedron (both Ni—O_{axial} distances are identical). Small chains of **B** appear to be retained in solution.¹²

The lack of examples of five-coordinate nickel in a mixed hard/soft (N/S) donor environment and the tendency for a spontaneous conversion from square planar, four-coordinate to octahedral, six-coordinate geometry in these cases has been suggested as a possible fundamental factor for substrate binding in nickel-containing enzymes.^{13–16} The following report chronicles exploration of $(\text{bme-daco})\text{Ni}^{\text{II}}$ and $(\text{bme}^*\text{-daco})\text{Ni}^{\text{II}}$ functionalized at sulfur with yet other potential axial O-donors, alcohol and alkoxide.

Experimental Section

General Procedures. Where anaerobic conditions were required, standard Schlenk techniques using nitrogen (passed through a drying tube of CaSO_4 , molecular sieves, and NaOH) and an argon glovebox (Vacuum Atmospheres) were employed. Solvents were dried and isolated under N_2 according to published procedures.¹⁷ Acetonitrile was distilled once from CaH_2 and twice from P_2O_5 and was freshly distilled from CaH_2 immediately before use. The following starting materials were of reagent grade and used as received: 2-iodoethanol (Aldrich), 1,3-dibromo-2-propanol (Aldrich), ammonium cerium(IV) nitrate (Strem), NaBH_4 (Aldrich), and NaOH (Mallinckrodt). NMR solvents were purchased in sealed ampules from Cambridge Isotope Laboratories and used as received.

Physical Measurements. UV–visible spectra were measured with a Hewlett Packard 8452A diode array spectrophotometer and quartz cells of light path length 1.00 cm. Cyclic voltammograms were recorded on a BAS-100A electrochemical analyzer using $\text{Ag}^0/\text{AgNO}_3$ reference and glassy carbon working electrodes with 0.1 M tetra-*n*-butylammonium hexafluorophosphate in CH_3CN or Ag^0/AgCl reference and glassy carbon working electrodes with 0.1 M KCl in methanolic solutions. EPR data on frozen solutions were obtained at 10 K on a Bruker ESP 300 spectrometer equipped with an Oxford Instruments ER910A cryostat. Elemental analyses were carried out by Galbraith Laboratories, Knoxville, TN. Magnetic susceptibility measurements were performed on an Evans balance purchased from Johnson Matthey Co. and by the Evans method¹⁸ on a Varian XL-200 FT-NMR spectrometer. X-ray crystallographic data were obtained on a Nicolet R3m/V single-crystal X-ray diffractometer or on a Rigaku AFC5-R diffractometer.

Syntheses. The $(\text{bme-daco})\text{Ni}^{\text{II}}$ and $(\text{bme}^*\text{-daco})\text{Ni}^{\text{II}}$ complexes were synthesized according to the published procedures with the following modifications.^{8,10} The $(\text{bme-daco})\text{Ni}^{\text{II}}$ complex was used as isolated following purification by silica column chromatography and removal of methanol via vacuum.

(*N,N'*-Bis(5-hydroxy-3-thiopentyl)-1,5-diazacyclooctane-*O,N,N',S,S'*)chloronickel(II), 1, and (*N,N'*-Bis(5-hydroxy-3-thiopentyl)-1,5-diazacyclooctane-*N,N',S,S'*)nickel(II) Iodide, 2. A 100 mg portion (0.344 mmol) of $(\text{bme-daco})\text{Ni}^{\text{II}}$ was dissolved in dry acetonitrile (50 mL), and 2 equiv of 2-iodoethanol (0.05 mL) was added via syringe. This solution was stirred under N_2 for 48 h at 50 °C, resulting in a color change from purple to brown. The solvent was removed by vacuum to a minimal volume. A double-tube arrangement for the diffusion of diethyl ether into this solution afforded two sets of crystals suitable for single X-ray analysis, blue **1** (trace amounts) and red-brown **2**. The optimum yield of **2** (ca. 60%) required 2 weeks, and single crystals of **1** appeared at the solution surface only after 1 week. These crystals were manually separated. Anal. Calcd (found) for **2**, $\text{C}_{14}\text{H}_{30}\text{N}_2\text{O}_2\text{S}_2\text{NiI}_2$: C, 26.5 (27.0); H, 4.44 (4.72); N, 4.41 (4.61). Electronic spectrum of **2** in MeOH [λ_{max} , nm (ϵ): 482 (212); in DMF: 486 (287)]. IR(KBr) of **1**: ν [cm^{-1}] = 3393, 3155, 1058. IR(KBr) of **2**: ν [cm^{-1}] = 3321, 1053.

(5-Hydroxy-3,7-dithianonediy)l-1,5-diazacyclooctane-*O,N,N',S,S'*)bromonickel(II) Bromide, 3. To $(\text{bme-daco})\text{Ni}^{\text{II}}$ (100 mg, 0.344 mmol) dissolved in 25 mL dry acetonitrile, was added 5 equiv of 1,3-dibromo-2-propanol (0.17 mL, 1.8 mmol) via syringe. The purple solution was stirred under N_2 until the color changed to brown. Slow diffusion of ether into the reaction mixture gave blue paramagnetic crystals suitable for single X-ray analysis (yield, 72.3%). Anal. Calcd (found) for $\text{C}_{13}\text{H}_{26}\text{N}_2\text{S}_2\text{ONiBr}_2$: C, 30.7 (31.0); H, 5.15 (5.04). Electronic spectrum in MeCN [λ_{max} , nm (ϵ): 382 (119), 598 (87); in H_2O : 486 (159)]. IR(KBr): ν [cm^{-1}] = 3428, 2959, 1062. $\mu_{\text{eff}} = 3.07 \mu_{\text{B}}$.

((5-Hydroxy-2,2,8,8-tetramethyl-3,7-dithianonediy)l-1,5-diazacyclooctane-*N,N',S,S'*)nickel(II) Bromide, 4. To *N,N'*-bis(2-methyl-2-mercaptopropyl)-1,5-diazacyclooctanenickel(II), $(\text{bme}^*\text{-daco})\text{Ni}^{\text{II}}$ (67.5 mg, 0.119 mmol), dissolved in 15 mL of dry acetonitrile was added 9 equiv of 1,3-dibromo-2-propanol (0.50 mL, 1.07 mmol) via syringe. The purple solution was stirred for 2 min and then set aside under N_2

(12) Goodman, D. C.; Farmer, P. J.; Reibenspies, J. H.; Darensbourg, M. Y. *Inorg. Chem.*, in press.

(13) Cha, M.; Gatlin, C. L.; Critchlow, S. C.; Kovacs, J. A. *Inorg. Chem.* **1993**, *32*, 5868.

(14) Ram, M. S.; Riordan, C. G.; Ostrander, R.; Rheingold, A. L. *Inorg. Chem.* **1995**, *34*, 5884.

(15) Sacconi, L. In *Transition-Metal Chemistry*; Carlin, R. L., Ed.; Dekker: New York, 1968; Vol. 4.

(16) Sacconi, L.; Mani, F.; Bencini, A. In *Comprehensive Coordination Chemistry*; Wilkinson, G., Gillard, R. D., McCleverty, J. A., Eds; Pergamon: New York, 1987; Vol. 5.

(17) Gordon, A. J.; Ford, R. A. *The Chemist's Companion*; Wiley and Sons: New York, 1972; pp 429–436.

(18) Evans, D. F. *J. Chem. Soc.*, **1959**, 2003.

Table 1. Crystallographic Summary for Structures 1–4

	1	2	3	4·2CH ₃ CN
chem formula	C ₁₄ H ₃₀ N ₂ O ₂ S ₂ NiCl	C ₁₄ H ₃₀ N ₂ O ₂ S ₂ NiI ₂	C ₁₃ H ₂₆ N ₂ OS ₂ NiBr ₂	C ₂₁ H ₄₀ N ₄ OS ₂ NiBr ₂
fw (g/mol)	543.58	635.0	509.0	647.22
space group	monoclinic <i>P2₁/n</i> (No. 14)	orthorhombic <i>Pca2₁</i> (No. 29)	orthorhombic <i>Pca2₁</i> (No. 29)	monoclinic <i>P2₁/c</i> (No. 13)
<i>a</i> (Å)	12.580(6)	15.822(2)	15.202(5)	20.348(5)
<i>b</i> (Å)	12.291(6)	13.171(2)	7.735(2)	6.5120(1)
<i>c</i> (Å)	13.090(7)	10.039(1)	15.443(4)	20.548(5)
β (deg)	97.36(4)			92.94(2)
<i>V</i> (Å ³)	2007(2)	2091(1)	1815.9(9)	2719(1)
<i>Z</i>	4	4	4	4
ρ (calc.) (g cm ⁻³)	1.799	2.016	1.862	1.581
temp (°C)	-80	23	-80	-110
radiation (λ , Å)			Mo K α (0.710 73)	
total no. of reflns	3896	2132	1656	4942
	$I \geq 2.0\sigma(I)$	$I \geq 2.0\sigma(I)$	$I \geq 2.0\sigma(I)$	$I \geq 2.0\sigma(I)$
no. of obsd reflns ^a	3528	1963	1656	4802
μ (cm ⁻¹)	0.2855	0.4054	0.5655	0.3826
<i>R</i> (%) ^a	6.71	3.26	3.53	9.94
<i>R_w</i> (%) ^a		3.01	3.36	
<i>R_w</i> (<i>F</i> ²) (%) ^a	18.34			20.16
<i>S</i> ^a		2.93	2.43	
<i>S</i> (<i>F</i> ²) ^a	1.06			1.10

^a Residuals: $R_{\text{int}} = [\sum F^2 - (F_{\text{mean}})^2]/[\sum F^2]$; $R = \sum |F_o - F_c|/\sum F_o$; $R_w = \{[\sum w(F_o - F_c)^2]/[\sum w(F_o^2)]\}^{1/2}$; $S = \{[\sum w(F_o - F_c)^2]/[N_{\text{data}} - N_{\text{parameters}}]\}^{1/2}$; $R_w(F^2) = \{[\sum w(|F_o^2| - |F_c^2|)^2/\sum w(F_o^2)^2]\}^{1/2}$; $S(F^2) = \{[\sum w(F_o^2 - F_c^2)^2]/[N_{\text{data}} - N_{\text{parameters}}]\}^{1/2}$.

until the color changed to brown-orange. Slow diffusion of diethyl ether into the reaction mixture gave orange crystals suitable for X-ray analysis (yield, 75%). Anal. Calcd. (found) for C₁₇H₃₄N₂O₂NiBr₂·2H₂O: C, 34.0 (33.3); H, 6.37 (6.37); N, 4.66 (4.47). Electronic spectrum in MeOH [λ_{max} , nm (ϵ): 288 (10341), 452 (225)]. IR(KBr): ν [cm⁻¹] = 3420, 2964, 1059.

Reduction of 3. Under anaerobic conditions, a Schlenk flask was charged with 10 mg of **3** and 20 mL of MeCN was added via syringe. To 10 mL of this blue stock solution was added 10 mL of 0.03 M NaBH₄ in EtOH by syringe. The color changed immediately to purple and then to green. An EPR sample was then taken from the green solution and frozen in N₂(l).

X-ray Crystallography and Structure Solution. All structures were solved at the Crystal & Molecular Structure Laboratory, Center for Chemical Characterization and Analysis at Texas A&M University. Crystallographic data for all complexes are listed in Table 1. A blue parallelepiped (0.18 mm × 0.22 mm × 0.36 mm) of **1** was mounted on a glass fiber with epoxy cement at room temperature and cooled to 193 K in a N₂ cold stream. Preliminary examination and data collection were performed on a Nicolet R3m/V X-ray diffractometer. Cell parameters were calculated from the least-squares fitting of the setting angles for 25 reflections with $2\theta > 15.0^\circ$. Lorentz and polarization corrections were applied to 3896 reflections. A semiempirical absorption correction was applied. A total of 3528 unique reflections were used in further calculations. The structure was solved by direct methods [SHELXS, SHELXTL-PLUS] with full-matrix least-squares anisotropic refinement on *F*² for all non-hydrogen atoms.¹⁹ Hydrogen atoms were placed in idealized positions with isotropic thermal parameters fixed at 0.80 Å. Despite the synthetic route which offers no obvious source of chloride, the sixth ligand in the structure of **1** is best modeled as chloride.

A red-brown parallelepiped (0.14 mm × 0.26 mm × 0.48 mm) of **2** was mounted on a glass fiber with epoxy cement at room temperature. Data were collected as for **1** with the following distinctions. Lorentz and polarization corrections were applied to 2132 reflections. A total of 1963 unique reflections were used in further calculations. The structure was solved by direct methods [SHELXS, SHELXTL-PLUS] with full-matrix least-squares anisotropic refinement for all non-hydrogen atoms.^{19a} Hydrogen atoms were placed in idealized positions with isotropic thermal parameters fixed at 0.80 Å.

A blue parallelepiped (0.20 mm × 0.20 mm × 0.50 mm) of **3** was mounted on a glass fiber with epoxy cement at room temperature and cooled to 193 K in a N₂ cold stream. Data were collected as for **1** with the following distinctions. Lorentz and polarization corrections were applied to 1656 reflections. A total of 1533 unique reflections were used in further calculations. The structure was solved by a Patterson synthesis [SHELXS, SHELXTL-PLUS] with full-matrix least-squares anisotropic refinement for all non-hydrogen atoms.^{19a} Hydrogen atoms were placed in idealized positions with isotropic thermal parameters fixed at 0.80 Å.

An orange needle of **4** (0.2 mm × 0.1 mm × 0.1 mm) was mounted on a glass fiber with epoxy cement at room temperature and cooled to 163 K in a N₂ cold stream. Data were collected as for **3** with the following distinctions. Preliminary examination and data collection were performed on a Rigaku AFC5-R diffractometer. Lorentz and polarization corrections were applied to 4942 reflections. A total of 4802 unique reflections were used in further calculations. The structure was solved by a Patterson synthesis [SHELXS, SHELXL-93] with full-matrix least-squares anisotropic refinement on *F*² for all non-hydrogen atoms.^{19b}

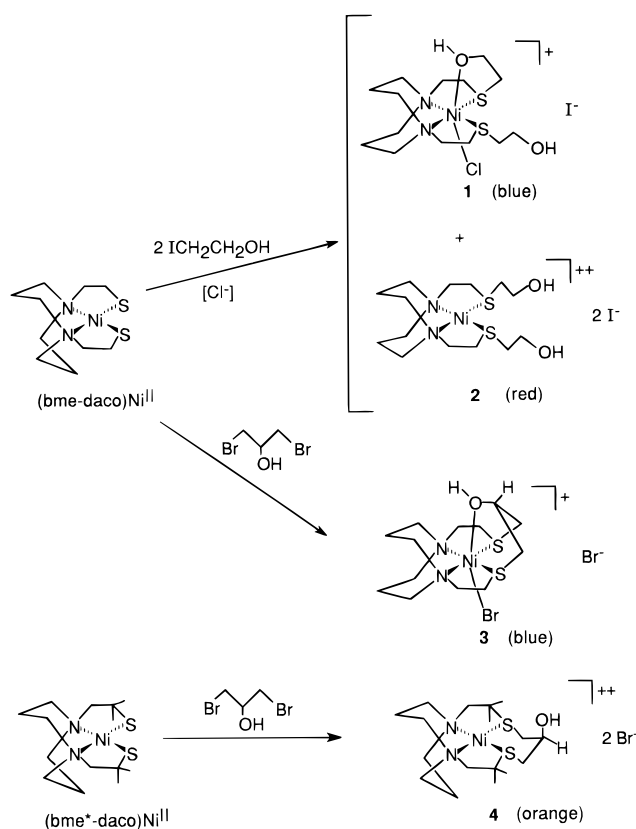
Results and Discussion

A summary of synthetic and coordination geometry results is found in Scheme 1. Complexes **1–4** have been characterized by X-ray crystallography; experimental crystallographic data are found in Table 1 and a comparison of selected bond lengths and bond angles in Table 2. Figures 1–4 present the molecular structures of complexes **1–4**, respectively.

The reaction of (bme-daco)Ni^{II} with stoichiometric amounts of ICH₂CH₂OH in CH₃CN affords dialkylated products; the monoalkylated species is not observed, as has been the case with previous alkylations.⁹ Two sets of crystals were obtained from ether diffusion and separated by hand. The minor (trace) product, **1**, is blue, the typical color of hexacoordinate Ni^{II} in a N, S, and O donor environment.^{9,11} The major product, **2**, contains Ni^{II} in a four-coordinate, square planar geometry with an N₂S₂ donor set, consistent with its red-brown color. Attempts to interconvert **1** and **2** have thus far been unsuccessful. Complex **2** is soluble only in polar solvents such as H₂O, EtOH, and MeOH, which maintain the hydroxy arm off and counterion separation. Careful examination of the crystal structure of **1** (*vide infra*) found the best structural refinement obtained by modeling the halide ligand *trans* to hydroxy as chloride rather

(19) (a) Sheldrick, G. M. SHELXTL-PLUS. Institut für Anorganische Chemie der Universität, Göttingen, Germany, 1988. (b) Sheldrick, G. M. SHELXL-93. Institut für Anorganische Chemie der Universität, Göttingen, Germany, 1993.

Scheme 1

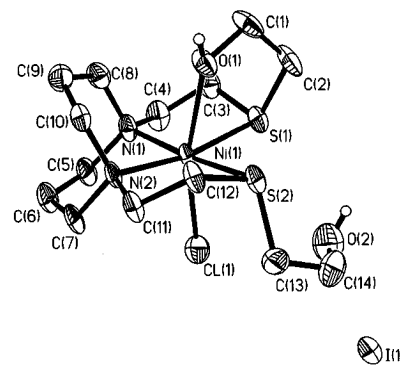
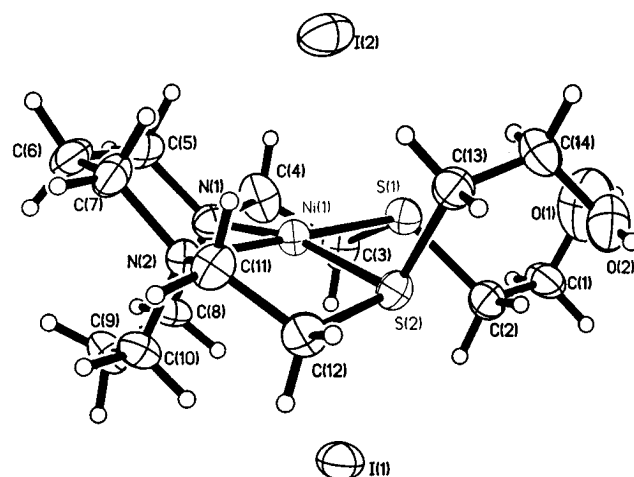
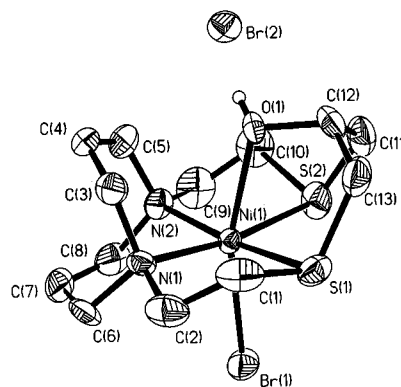
**Table 2.** Selected Bond Lengths (Å), Angles (deg), and Tetrahedral Twist (deg) for 1–4

	1	2	3	4
Ni(1)–N(1)	2.101(6)	1.974(7)	2.088(7)	1.98(2)
Ni(1)–N(2)	2.110(6)	1.970(7)	2.060(7)	1.97(2)
Ni(1)–S(1)	2.400(2)	2.207(3)	2.390(3)	2.174(7)
Ni(1)–S(2)	2.444(2)	2.213(3)	2.380(3)	2.143(6)
Ni(1)–O(1)	2.293(6)		2.270(7)	
Ni(1)–X ^a	2.465(2)		2.510(2)	
N(1)–Ni(1)–N(2)	85.6(2)	88.8(3)	86.1(3)	92.1(8)
S(1)–Ni(1)–S(2)	95.7(8)	91.0(1)	93.5(1)	92.5(3)
S(1)–Ni(1)–N(1)	88.6(2)	89.5(2)	89.2(2)	87.3(6)
S(1)–Ni(1)–N(2)	169.7(2)	178.3(2)	169.7(3)	175.1(6)
S(2)–Ni(1)–N(1)	170.5(2)	167.3(2)	171.5(2)	175.4(6)
S(2)–Ni(1)–N(2)	88.9(2)	90.6(2)	89.9(2)	87.7(6)
O(1)–Ni(1)–S(1)	77.9(2)		77.7(2)	
O(1)–Ni(1)–N(1)	96.1(3)		95.1(3)	
O(1)–Ni(1)–X ^a	164.2(2)		162.3(1)	
X ^a –Ni(1)–S(1)	90.1(7)		88.5(1)	
X ^a –Ni(1)–N(1)	93.9(2)		95.6(2)	
Td twist	3.3	12.7	3.2	6.8

^a X = Cl in complex 1; X = Br in complex 3.

than iodide. Since all attempts to increase the yield of **1** by providing an external source of Cl⁻ were unsuccessful, we tentatively conclude that adventitious chloride is introduced during column chromatography of the parent (bme-daco)Ni^{II} complex. An alternate model of the structure defining the axial halide as iodide could only be refined if I(2) were present in 39% occupation and an unrealistic distance of 2.465 Å from the Ni^{II} center. In fact, such a distance is normal for Ni–Cl.²⁰

Molecular Structures. Complex **1**, Figure 1, contains nickel in a slightly distorted octahedral coordination environment. Five donor atoms of the hexadentate ligand are bound to Ni^{II}, as well

**Figure 1.** Crystal structure of **1** (thermal ellipsoids at 50% probability).**Figure 2.** Crystal structure of **2** (thermal ellipsoids at 50% probability).**Figure 3.** Crystal structure of **3** (thermal ellipsoids at 50% probability).

as Cl(1), which is 2.465(2) Å away from the Ni center, and *trans* to O(1). This Ni–X distance is typical of (Ni–Cl)_{av} and 0.29 Å shorter than (Ni–I)_{av}.²⁰ The other alcohol arm is found unbound and oriented on the same side of the N₂S₂ plane as Cl(1). The second I⁻ ion, I(1), resides in the region of the OH group bound to the Ni with a I–O distance of 3.41 Å. This distance, combined with an observed solid state H–O IR band at 3155 cm⁻¹, suggests the iodide is linked by a hydrogen bond to the ethanolic proton attached to the oxygen atom bound to the nickel center. The O–Ni–Cl(1) bond angle is 164.2°. The Ni–S(1)–C(13) bond angle is 112.1(3)°. However, the dangling arm has a Ni–S(2)–C(2) bond angle of 100.9(3)°.

Complex **2**, Figure 2, is square planar with the Ni located in the N₂S₂ plane. The closest iodide ions in the crystal lattice, I(1) and I(2) are located 4.060 and 3.542 Å from the Ni center, respectively. As in **1**, the ethylene links from N to S are eclipsed, and the unbound hydroxyethyl arms are found in an *anti* configuration with respect to the NiN₂S₂ plane. The Ni–

(20) Orpen, A. G.; Brammer, L.; Allen, F. H.; Kennard, O.; Watson, D. G.; Taylor, R. J. *Chem. Soc., Dalton Trans.* **1989**, S.1.

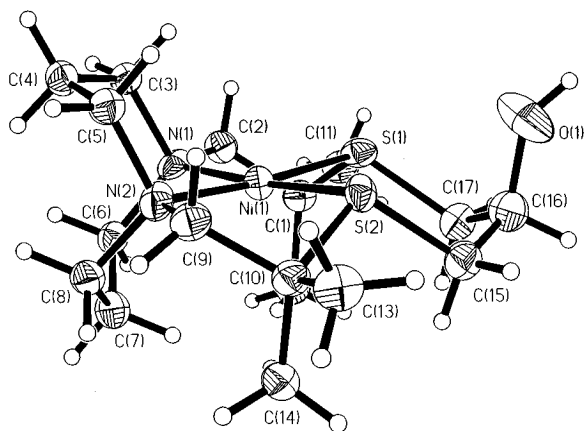


Figure 4. Crystal structure of **4** (thermal ellipsoids at 50% probability).

S(1)–C(2) bond angle is opened by 5° as compared to the Ni–S(2)–C(13) bond angle, 115.5(3) and 110.2(3)°, respectively. Both are larger than the 108.0(4)° Ni–S–C angles found in the [(Me₂bme-daco)Ni][I]₂ complex in which the methyl groups are in a *syn* configuration.⁸ As observed with other S-derivatives of (bme-daco)Ni^{II}, the N₂S₂ cavity of hexacoordinate **1** is larger than that of tetracoordinate **2**; the Ni–S bond lengths are *ca.* 0.2 Å longer and the Ni–N bonds *ca.* 0.13 Å longer in complex **1** as compared to **2**.^{9–11} This result of increasing the number of electron pairs around the Ni center from four to six is consistent with metric data of the four-coordinate [Ni(bme*-ether)]I₂ and the six-coordinate [Ni(bme-ether)]I complexes described above.^{10,11} There is a slight tetrahedral twist in the N₂S₂ plane of **2** as defined by the angle of intersection of the normals to the Ni–S(1)–S(2) and Ni–N(1)–N(2) planes.

The binding of a metal to the diazacyclooctane ligand fragment results in the formation of two metallodiazacyclohexane rings whose conformations are dependent upon the coordination sphere of the metal. Typically, four-coordinate complexes exist with the rings in the chair/boat conformation, whereas in six-coordinate complexes the rings are in the chair/chair conformation.^{8–10,21} The latter is found for complexes **1** and **3** and, unexpectedly, for complex **2**. Although molecular modeling calculations showed little difference between the chair/boat and chair/chair conformations of the diazacyclohexane rings, **2** is only the second four-coordinate complex to be found in the chair/chair conformation.^{11,22} There is no obvious intermolecular packing arrangement which accounts for this.

Alkylation of (bme-daco)Ni^{II} with 1,3-dibromo-2-propanol resulted in the formation of a N₂S₂O pentadentate macrocyclic complex **3**. Diethyl ether diffusion into a CH₃CN solution yielded blue crystals suitable for X-ray analysis. The molecular structure of **3**, Figure 3, exhibits the Ni^{II} center in an octahedral environment of the N₂S₂O donor set completed by a halide ion. Once again, the Ni is in the N₂S₂ plane with an axial Ni–O bond length of 2.270(7) Å and a Ni–Br distance of 2.510(2) Å. The Ni–O length is slightly shorter than that observed in [Ni(bme-ether)]BPh₄, 2.387(5) Å,¹¹ and *ca.* 0.2 Å longer than the Ni–O bond in complex **1**.⁹ The O–Ni–Br(1) bond angle is 162.3(12)°, only 1.9° smaller than the O–Ni–Cl(1) angle in **1**. The Ni–S and Ni–N distances are similar to those of **1**, *i.e.*, elongated by 0.2 and 0.1 Å, respectively, over those of four-coordinate analogs. An additional similarity between complexes **1** and **3** is that the Ni–S(1)–C(13) bond angles are both 100.9(3)°.

Table 3. Physical/Spectroscopic Data for Complexes **2–4**

complex	form/color solid/ MeCN/H ₂ O or MeOH	UV–vis λ, nm (ε)	μ _{eff} , BM ^a 20 °C
2	red/insoluble/red-brown	482 (212) ^b 486 (287) ^c	2.54
2a	.../.../green	380 (2232) ^d	3.04 ^e
3	blue/blue/red-brown	382 (119), 598 (87) ^f 486 (159) ^g	3.07
4	orange/orange/orange	452 (225) ^b	2.68 ^e

^a Except where noted, in the solid state. ^b MeOH solution. ^c DMF solution. ^d DMF:H₂O solution. ^e Evans solution NMR method, data collected on **2** in the presence of *xs* NaOH. ^f MeCN solution. ^g H₂O solution.

Complex **4**, prepared and isolated similarly to **3**, contains Ni^{II} in four-coordinate, square planar geometry with two bromides as counterions and two acetonitrile molecules in the crystal lattice. This lack of axial coordination in **4** is caused by the steric hindrance of the four methyl groups α to the sulfur. As observed with other four- and six-coordinate analogs, the Ni–N bonds are *ca.* 0.1 Å shorter in four-coordinate **4** than in six-coordinate **3** and the Ni–S bonds are 0.22 Å shorter than in **3**. The N(1)–Ni–N(2) bond angle of **4** (92°) is 6° wider than that in **3** (86°); the S(1)–Ni–N(2) angle also opens by 5° in **4**.

As seen in Figure 4, the newly formed nickel-2,6-dithia-cyclohexane ring adopts a chair conformation with the hydroxyl group occupying an axial position on the six-membered ring. Hydrogen bonding between the alcoholic hydrogen and the bromide counterion can be viewed as stabilization of the chair conformation of this metallocycle. On the other hand, an analogous complex, [Ni(bme*-ether)]I₂, *vide supra*, has shown that the conformation of the thioether rings in the solid state can be strictly a result of packing forces. In the case of [Ni(bme*-ether)]I₂, the eight-membered metallo thioether/ether ring adopts a boat/boat (saddle) conformation in which the distance between the nickel and the ether oxygen is 2.431(5) Å, *i.e.*, 0.044 Å beyond the bonding distance established for [Ni(bme-ether)]BPh₄.¹⁰ In complex **4**, the Ni–S_{thioether} distances are shorter (0.03–0.06 Å) than expected for the previously structured four-coordinate thioether derivatives of (bme*-daco)-Ni^{II} and 0.025 Å shorter than the Ni–S distances in **2**. Thus, the steric effect provided by the four methyl groups in (bme*-daco) does not lengthen the Ni–S bonds.

Spectroscopy. Spectroscopic and certain physical properties of these compounds are listed in Table 3. Typically, four-coordinate derivatives of (daco-bme)Ni^{II} display red hues, and six-coordinate species appear blue.^{9–11} Unfortunately, the colors of their solutions are solvent dependent. Complex **2** is four coordinate in all solvents in which it is soluble and remains red-brown. Complex **4**, like other tetracoordinate (bme*-daco)-Ni^{II} thioether derivatives, exhibits an orange color in methanol as well as in acetonitrile.¹⁰ As observed for six-coordinate nickel complexes with O donors, **3** is blue; the color persists in MeCN, but turns red-brown in H₂O. Addition of aliquots of H₂O to a solution of **3** in MeCN until the H₂O comprises 4% total volume produces a color change from blue to purple to red-brown. The overlaid UV–vis spectra, Figure 5, show absorptions at 592 and 382 nm diminishing and an absorption at 500 nm increasing. The absorptions at 592 and 382 nm correspond to the octahedral ³A_{2g} → ³T_{2g} (ν₁) and ³A_{2g} → ³T_{1g} (ν₂) d–d transitions, respectively. The ν₃ band at higher energy is obscured by a charge transfer band *ca.* 330 nm.²³ From this data, it is inferred that a coordination sphere conversion (from six- to four-coordinate) occurs as water solvates the halide ions.

(21) Musker, W. K.; Hussain, M. S. *Inorg. Chem.* **1966**, *5*, 1416.

(22) Tuntulani, T.; Musie, G.; Reibenspies, J. H.; Darensbourg, M. Y. *Inorg. Chem.* **1995**, *34*, 6279.

(23) Ballhausen, C. J. *Adv. Chem. Phys.* **1963**, *5*, 33.

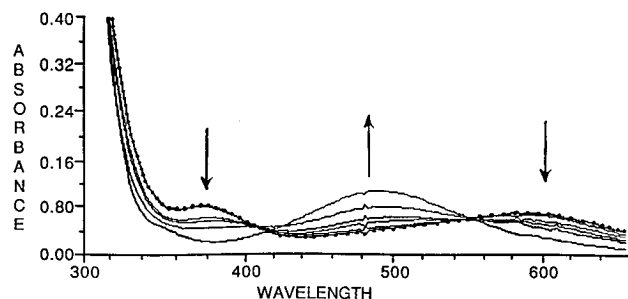


Figure 5. UV-vis spectra of **3** in CH_3CN (···) and overlaid spectra obtained on addition of aliquots of H_2O to **3** until H_2O comprises 4% of total volume (isobestic points: 424 and 556 nm).

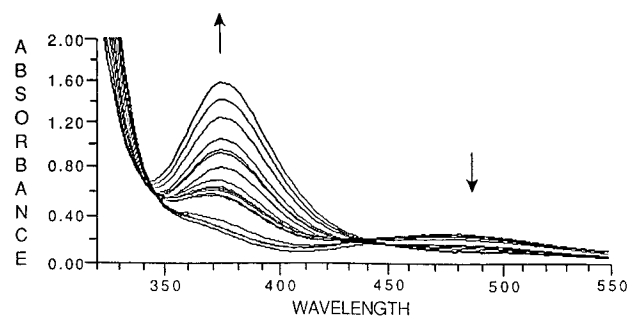
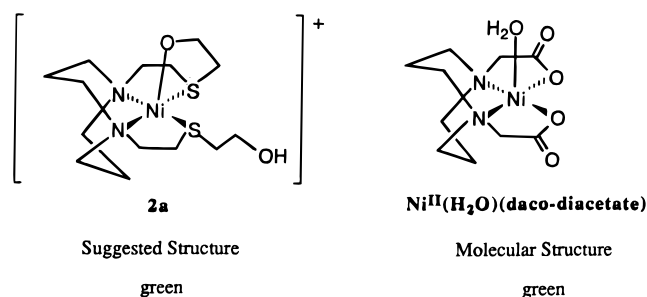


Figure 6. Overlaid UV-vis spectra of **2** in DMF and **2** following addition of aliquots of 0.49 M NaOH up to 2 equiv (isobestic point: 444 nm).

In excess base, **2** changes into a green material, presumably deprotonated **2**, represented as **2a** below. This green species, which displays a characteristic band at 380 nm in the UV-vis, has not succumbed to crystallization techniques. On the basis of the green $\text{Ni}^{\text{II}}(\text{H}_2\text{O})(\text{daco-diacetate})$ complex reported by Legg *et al.*, **2a** is assumed to be an analogous pentacoordinate



complex.²⁴ An attempt to determine the $\text{p}K_{\text{a}}$ of **2** by potentiometric titration was carried out by addition of a 0.102 M KOH solution to an aqueous solution of **2**. Results indicate that the $\text{p}K_{\text{a}}$ of the ethanolic proton is higher than 11, *i.e.*, above the practical technique limit.²⁵ Spectrophotometric data were obtained with successive addition of aqueous 0.49 M NaOH to a solution of **2** in DMF. The DMF: H_2O ratio was maintained at 97:3; $k_{\text{w}} = 1 \times 10^{-16}$ in DMF.²⁶ The overlaid spectra (Figure 6) show the disappearance of the absorption for **2** at 486 nm ($\epsilon = 268 \text{ L mol}^{-1} \text{ cm}^{-1}$) and the concomitant appearance of **2a** at 380 nm ($\epsilon = 2232 \text{ L mol}^{-1} \text{ cm}^{-1}$). An isobestic point at 444 nm indicates the formation of a single new species. A plot of the absorbance at 380 nm vs moles of base added yields a titration curve as well as the molar absorptivity coefficient, $\epsilon_{2\text{a}}$.

(24) (a) Nielson, D. O.; Larsen, M. L.; Willett, R. D.; Legg, J. I. *J. Am. Chem. Soc.* **1971**, *93*, 5079. (b) Averill, D. F.; Legg, J. I.; Smith, D. L. *Inorg. Chem.*, **1972**, *11*, 2344. (c) Legg, J. I.; Nielson, D. O.; Smith, D. L.; Larsen, M. L. *J. Am. Chem. Soc.* **1968**, *90*, 5030. (d) Kanamori, K.; Broderick, W. E.; Jordan, R. F.; Willett, R. D.; Legg, J. I. *J. Am. Chem. Soc.* **1986**, *108*, 7122.

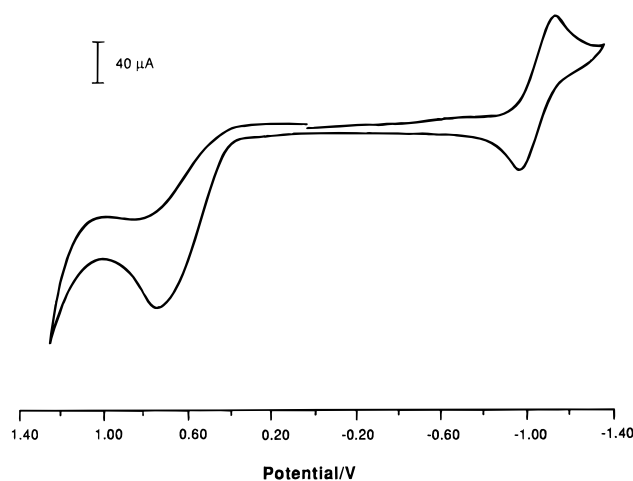


Figure 7. Cyclic voltammogram of **2** (2 mM) in MeOH. Conditions: saturated methanolic solution of KCl; $E_{1/2} = -1072 \text{ mV}$ (vs NHE), with $\Delta E_{\text{a/c}} = 88 \text{ mV}$ and $i_{\text{pa}}/i_{\text{pc}} = 0.93$.

Using the spectrophotometric data and eqs 3–6 the $\text{p}K_{\text{a}}$ value

$$[\text{total}] = [\mathbf{2}] + [\mathbf{2a}] \quad (3)$$

$$\text{abs}_{380} = \epsilon_2[\mathbf{2}] + \epsilon_{2\text{a}}[\mathbf{2a}] \quad (4)$$

$$\text{abs}_{380} = \epsilon_2[\mathbf{2}] + \epsilon_{2\text{a}}([\text{total}] - [\mathbf{2}]) \quad (5)$$

$$K_{\text{a}} = [\mathbf{2a}][\text{H}^+]/[\mathbf{2}] \quad (6)$$

was calculated to be 13.9. This is within the reported range for the $\text{p}K_{\text{a}}$ of an alcoholic proton in DMF ($\text{p}K_{\text{a}} = 13.85\text{--}14.34$).²⁷ Loss of the proton is not promoted by O-binding to the Ni center. The pronounced increase in the value of $\epsilon_{2\text{a}}$ further substantiates the formation of a new species with a less centrosymmetric geometry. On changing from four- to five-coordinate complexes, the otherwise Laporte-forbidden transitions become allowed, thereby increasing the observed intensity of the absorption band.

The magnetic moment was determined via the Evans method^{18,28} to be $2.54 \mu_{\text{B}}$ for **2** and $3.04 \mu_{\text{B}}$ for **2a** in methanol; these results are consistent with the existence of two unpaired electrons in the complexes (calculated $\mu_{\text{s.o.}}$, $2.83 \mu_{\text{B}}$). These results together with the electrochemistry described below imply that in solution **2** remains four coordinate (O unbound) with a tetrahedral twist that is sufficient to unpair electrons, and under basic conditions, the coordination sphere changes to five, most likely a distorted square pyramid.

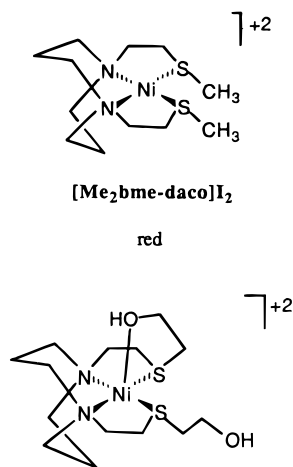
Electrochemistry. The cyclic voltammogram of **2** as the iodide salt in MeOH displays a cathodic event, presumed to be the $\text{Ni}^{\text{III/I}}$ couple, at $E_{1/2} = -1070 \text{ mV}$ referenced to NHE (Figure 7 and Table 4) and an irreversible oxidation at *ca.* 800 mV. No other oxidation waves were observed when **2** was scanned to 1400 mV. Although there is approximately a 2 V separation between the reduction and oxidation events as observed with other (bme-daco) Ni^{II} derivatives,^{3,11} the cyclic voltammogram of **2** is significantly different from those of analogous complexes without functionalized thioethers. Surprisingly, the cyclic voltammogram is most similar to that of a single alkylated species and is inconsistent with those of dialkylated complexes.^{3,10,11} The monoalkylated complexes exhibit reversible to quasi-reversible $\text{Ni}^{\text{III/I}}$ couples and an oxidation event, which may be ligand based, at *ca.* 2 V more positive potential; such is the case for solutions of **2**. Some possible rationale for this include the following: (1) one of the O atoms may interact with the Ni center thereby achieving pentacoordination and altering

Table 4. Redox Potentials^a and Reversibility Data from Cyclic Voltammetry of Complexes **2–4** (defined in Scheme 1)

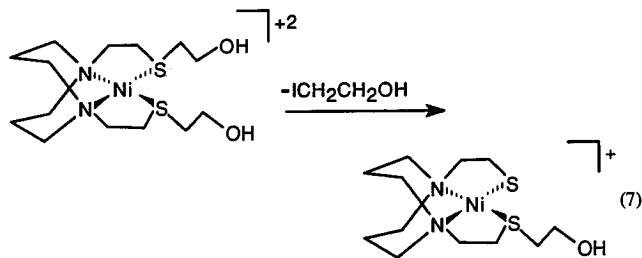
compound (solvent)	$E_{1/2}$ (mV)		i_{pa}/i_{pc}	ΔE (mV)
	Ni ^{III/II}	Ni ^{II/I}		
2 (DMF) ^b		-1306	0.73	66
2 (MeOH) ^c		-1070	0.84	84
3 (MeCN) ^b	1373	-749	1.07, 0.61	53, 106
3 (MeCN + 250 μ L of H ₂ O) ^b		-741	0.90	94
3 (MeCN + 400 μ L of H ₂ O) ^b		-733	0.96	94
3 (MeCN + 700 μ L of H ₂ O) ^b		-733	1.02	94
3 (H ₂ O) ^{c,d}		-693	0.77	73
4 (MeCN) ^b	1110	-664	0.36, 0.81	84, 15
[Ni(bicycle)]Br ₂ (MeCN) ^b		-766	0.79	76
[Ni(bicycle)]Br ₂ (H ₂ O) ^{c,d}		-609	1.00	78
[Ni(ether)]I (MeCN) ^b		-514	0.73	88

^a All potentials referenced to NHE with ferrocene as internal standard unless otherwise indicated; scan rate of 200 mV/s. ^b With glassy carbon vs Ag⁰/AgNO₃ electrodes, 0.1 M [*n*-Bu₄N][PF₆] as supporting electrolyte. ^c With glassy carbon vs Ag/AgCl electrodes, 0.1 M KCl as supporting electrolyte. ^d MeV²⁺/MeV⁺ as internal standard.

the redox properties of the Ni center;



(2) one of the ethanolic arms has been lost or displaced (eq 7). The Ni^I moiety in **2** is *ca.* 600 mV less accessible than that of [(Me₂bme-daco)Ni][I]₂ and 100 mV less accessible than that of [(Mebme-daco)Ni]I.³ Upon addition of base and the formation of **2a**, the Ni^{II/I} couple vanishes.



Complex **3** has a Ni^{II/I} reduction at -750 mV, and also displays a Ni^{III/II} oxidation at 1370 mV referenced to NHE (Figure 8 and Table 4). The effect of incremental aliquots of water on the electrochemistry of **3** was investigated. Complex

(25) Martell, A. E.; Motekaitis, R. J. *Determination and Use of Stability Constants*, VCH Publishers, Inc.: New York, 1992.

(26) Badoz-Lambling, J.; Demange-Guérin, G. *Bull. Soc. Chim. Fr.* **1964**, 1354.

(27) Izutsu, K. *Acid-Base Dissociation Constants in Dipolar Aprotic Solvents*; Blackwell Scientific Publications: Boston, MA, 1990; pp 41–63.

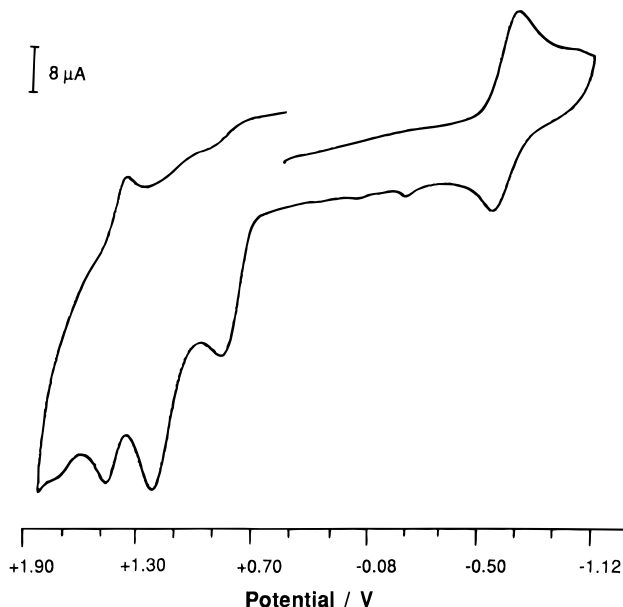
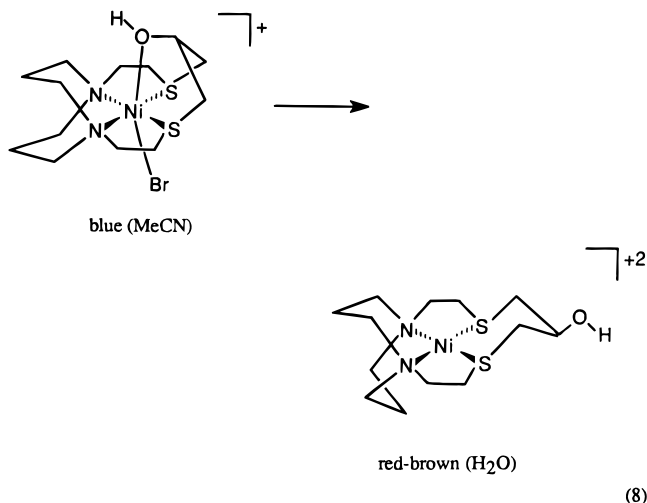


Figure 8. Cyclic voltammogram of **3** (2 mM) in MeCN. Conditions: 0.1 M [*n*-Bu₄N][PF₆]; for Ni^{II/I}, $E_{1/2} = -749$ mV (vs NHE), with $\Delta E_{a/c} = 53$ mV and $i_{pa}/i_{pc} = 1.07$; for Ni^{III/II}, $E_{1/2} = 1373$ mV (vs NHE), with $\Delta E_{a/c} = 106$ mV and $i_{pa}/i_{pc} = 0.61$.

3 was dissolved in 10 mL (1 mM) of 0.1M Bu₄NPF₆ in MeCN. While keeping the total volume constant, water was added incrementally up to 0.7 mL (eq 8). After each increase in H₂O,



a CV scan was performed and a UV-vis spectrum was taken. The cyclic voltammetry and UV-vis experiments performed on these solutions exhibited both a spectral change and an altered reduction potential. UV-vis results were the same as discussed earlier. The color changed from blue to purple, and the Ni^{II/I} reduction became both more reversible and slightly more accessible ($E_{1/2}$ went from -750 mV to -730 mV, ΔE from 106 mV to 94 mV, i_{pa}/i_{pc} from 0.605 to 1.021). The red-brown, four-coordinate species in water exhibits the loss of the Ni^{III/II} oxidation, and the Ni^{II/I} reduction becomes both more accessible and reversible, $E_{1/2} = -690$ mV, $\Delta E = 73$ mV, and $i_{pa}/i_{pc} = 0.77$.

A N₂S₂OX donor set which is similar to **3** is observed in [Ni(bme-ether)]I.¹¹ The molecular structure shown earlier is six-coordinate with a longer Ni-O bond distance (2.387(5) Å) as compared to the Ni-O bond length in **3** (2.290(6) Å). The

(28) Grant, Douglas *J. Chem. Educ.* **1995**, 72, 39.

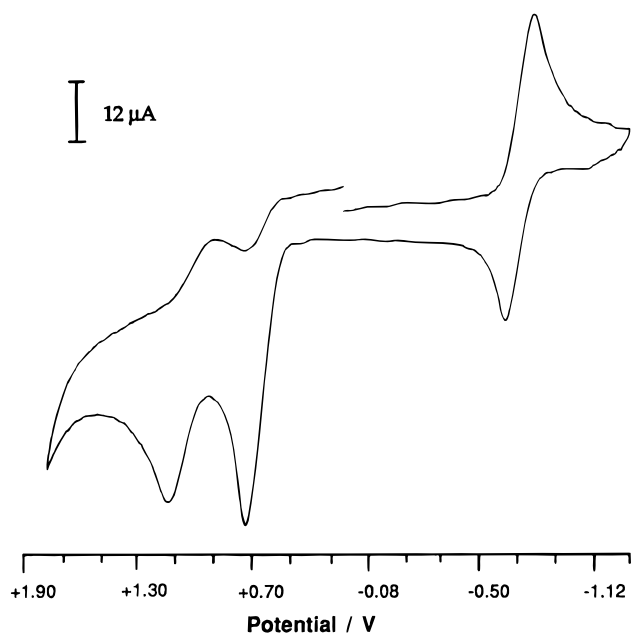


Figure 9. Cyclic voltammogram of **4** (2 mM) in MeCN. Conditions: 0.1 M $[n\text{-Bu}_4\text{N}][\text{PF}_6]$; for Ni^{II} , $E_{1/2} = -664$ mV (vs NHE), with $\Delta E_{\text{avc}} = 84$ mV and $i_{\text{pa}}/i_{\text{pc}} = 0.36$; for Ni^{III} , $E_{1/2} = 1110$ mV (vs NHE), with $\Delta E_{\text{avc}} = 15$ mV and $i_{\text{pa}}/i_{\text{pc}} = 0.81$.

green color of the ether complex in MeCN is taken as an indication of a pentacoordinate species or a six-coordinate complex with a weakly bound axial ligand. In contrast, the ion exchange product, $[\text{Ni}(\text{bme-ether})][\text{BPh}_4]_2$, is red (four-coordinate) in solution. The $[\text{Ni}(\text{bme-ether})\text{I}]\text{I}$ complex exhibits a Ni^{II} reduction at -515 mV in acetonitrile vs NHE. From this we surmise that in **3** the stronger interaction between the Ni and O is sufficient to hinder the formation of the Ni^{I} species. However, a $\text{Ni}^{\text{II/III}}$ oxidation has not been reported for $[\text{Ni}(\text{bme-ether})\text{I}]\text{I}$ in acetonitrile. This result further substantiates the expectation that axial ligation destabilizes the Ni^{I} oxidation state and stabilizes the Ni^{III} oxidation state. In general, four-coordinate compounds display greater accessibility to Ni^{I} than six-coordinate species because the added electron density on the Ni center in the latter causes an electrostatic destabilization in the axial direction (Jahn–Teller effect), thereby making the four-coordinate species a more favorable geometry for Ni^{I} . The converse holds true for Ni^{III} . Thus, the UV–vis and CV experiments are fully complementary with regards to coordination and geometry.

Complex **4** also exhibits both a Ni^{II} reduction and a $\text{Ni}^{\text{II/III}}$ oxidation, Figure 9 and Table 4. The quasi-reversible reduction couple occurs at -664 mV and the quasi-reversible oxidation at 1110 mV, referenced to NHE. The Ni center in **4** is *ca.* 85 mV easier to reduce than the Ni center in **3**. These results are consistent with the lower coordination number observed for the thioether derivatives of $(\text{bme}^*\text{-daco})\text{Ni}^{\text{II}}$ and thus the increase in accessibility of the Ni^{I} state relative to the $(\text{bme-daco})\text{Ni}^{\text{II}}$ derivatives.

Bulk chemical reduction of **3** in MeCN with NaBH_4 produces a color change to green, indicative of a coordination change to five.²⁴ A frozen sample of this solution exhibits an axial EPR signal, Figure 10, and calculated g values of 2.21 and 2.06, indicative of an unpaired electron in the $d_{x^2-y^2}$ orbital of a Ni^{I} species. Bulk oxidation of **3** with ammonium cerium(IV) nitrate did not result in an EPR-active species.

Additional evidence for the correlation between redox potentials and coordination environment have been reported earlier,^{8–11} the Ni^{II} redox potential for six-coordinate complexes

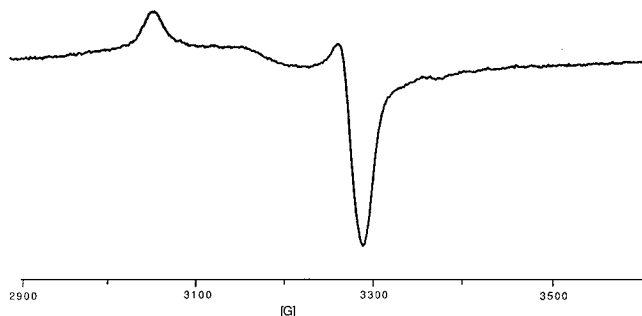
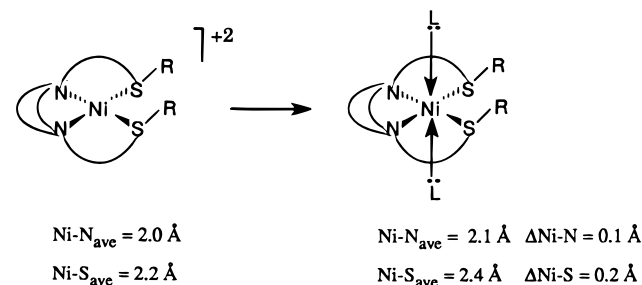


Figure 10. X-band EPR spectra, data collected at 10 K ($\nu = 9.441$ GHz) for **3** in MeCN (1 mM) after reduction with NaBH_4 . Calculated g values: 2.208, 2.06.

is significantly more negative than those of four-coordinate species (Table 4). Additionally, it has been reported that when heteroatoms are present in the ligand set, H-bonding may positively shift redox potentials as much as 200 mV in the absence of a coordination change.²⁹ Thus, one might argue that the O atoms in the complexes reported here are experiencing H-bonding in water, and thereby the redox potentials are shifting to more positive values. However, for the N_2S_2 macrocyclic complexes this trend is also observed.¹¹ Therefore, it may be concluded that the redox shifts are induced by a coordination number change.

Concluding Remarks

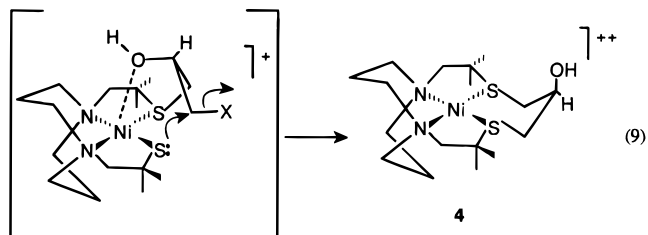
The derivatization of $(\text{bme-daco})\text{Ni}^{\text{II}}$ by the addition of ring forming agents containing an additional ligating site has proven to be a very effective way to generate macrocycles of increased denticity of known *cis* dithiolate complexes. Our work has extended demonstrations of nickel's propensity to avoid pentacoordination in a mixed hard/soft donor set. The six-coordinate complexes possessing a counterion in one of the axial positions may easily be converted to four-coordinate species by adding solvents that promote solvent separated ion pairs. The observed coordination chemistry of these complexes accounts for their variability in redox chemistry; four-coordinate species stabilize the Ni^{I} state whereas six-coordinate species tend to stabilize the Ni^{III} state and have less stable Ni^{I} moieties. This trend is also consistent with the metric parameters of the N_2S_2 cavity; six-coordinate species have a larger cavity as a result of the electronic destabilization incurred by adding two pairs of electrons to the metal center.



In order to account for the conformational preference of complex **4** (OH in the axial position with respect to the nickel thiacyclohexane ring), we suggest that in addition to the template effect,⁷ the $-\text{OH}$ can assist in the ring closure in a metal-directing effect that results in the observed stereochemistry. An interaction between the oxygen of the alcohol and the metal

(29) Huang, J.; Ostrander, R. L.; Rheingold, A. L.; Leung, Y.; Walters, M. A. *J. Am. Chem. Soc.* **1994**, *116*, 6769.

center would facilitate the nucleophilic attack of the thiolate sulfur on the C–X bond and would render the –OH axial once the ring is formed (eq 9). This mechanism is of course consistent with the molecular structure of **3** in which the –OH is bound to the nickel center.



Acknowledgment. Financial support from the National Science Foundation (Grant CHE 94-15901) is gratefully acknowledged. Funding for the X-ray diffractometer and crystallographic computing system (Grant CHE 8513273) was provided by the National Science Foundation. The authors wish to thank A. Clearfield for use of the AFC5-R diffractometer.

Supporting Information Available: Text summarizing the structure determination of refinement, tables summarizing crystallographic data, bond lengths and angles, atomic coordinates, anisotropic displacement parameters, and H-atom coordinates and packing diagrams for compounds **1–4** (23 pages). Ordering information is given on any current masthead page.

IC9514612